引用格式：YAO Dong，GAO Bo，SONG Yingzheng，et al. Research on Ultrasonic Response Characteristics of Structures Excited by Laser Transient Grating[J]. Acta Photonica Sinica，2022，51(9)：0914001
姚东，高波，宋英政，等. 激光瞬态光栅激励下结构的超声响应特性研究[J]. 光子学报，2022，51(9)：0914001

激光瞬态光栅激励下结构的超声响应特性研究

姚东[1,4]，高波[2]，宋英政[3]，李群[3]，高贵龙[4]

（1 火箭军工程大学，西安 710025）
（2 上海航天技术研究院，上海 200233）
（3 西安交通大学，西安 710049）
（4 中国科学院西安光学精密机械研究所，西安 710119）

摘　要：将脉冲激光的空间展开与激光超声无损检测相结合，数值分析及实验研究了激光瞬态光栅作用于铝合金板的结构响应。数值分析了反射-吸收综合模型框架下表面粗糙度对吸收率的影响，进行了直径 1 mm 外型、脉冲宽度 1 ns、单脉冲 6 mJ 输入下激光瞬态光栅激励过程的仿真，并开展了相同能量条件下束斑点光源、有限长度线光源的比对分析；数值分析结果表明，观测距离小于等于 4 mm 的范围内，瞬态光栅激发下峰值为点源激发的 2～5 倍，且结构表面能量密度约为点源模式的 1%、线源模式的 12.7%。开发了瞬态光栅模块并搭建了激发-检测实验系统，结合 49.36 mm×49.80 mm×4.97 mm 尺寸的铸铝平板进行了验证比对。实验结果表明，60 kHz 高通滤波下噪声幅值约为 1 nm，距离光栅中心位置 2 mm 处表面位移峰值的相对偏差最大值为 8.91%、10 mm 处信号时延对应的声表面波速度偏差为 6.62%。

关键词：超声无损检测；激光激发；栅形空间调制；能量密度；信号强度
中图分类号：O439　　**文献标识码**：A　　**doi**：10.3788/gzxb20225109.0914001

0 引言

超声无损检测支持现场使用且分辨能力强，是结构健康监检测领域重点发展的手段。近年来，相继形成了基于压电传感器的贴片检测、介质耦合检测、空气耦合检测等接触式技术路线，广泛应用于多个行业[1-5]。随着无接触、大范围等应用需求的涌现，以及高品质脉冲激光器技术与激光-物质作用机理研究[6-7]的融合，脉冲激光激发超声的检测技术逐步从实验室研究走向工程应用[8-11]，并发展了压电测量等半接触激光超声方案、激光测量等非接触激光超声方案。

激光超声检测的基本原理是激光与物质的相互作用：脉冲激光向结构传递能量，按能量传递后温度上升的程度，进一步分为热蚀效应和热弹效应；热蚀效应下，物质发生熔化甚至气化，表现为质量损失、局部结构缺损，而热弹效应下温度升高、能量积累的程度不足以产生融化或气化。脉冲激光激发的不足在于：激光的单色相干制约了束斑调制能力、导致了超声时频模式受限，结构损伤阈值则限制了脉冲激光的能量、导致超声信号强度的不足。苏琨、宋潮等相继结合实验比较了线光源与点光源所产生超声信号的差异[12-13]，证实了线源激发的优势。NISHINO H 采用 10 组分光-光纤模块得到了窄带且相移的阵列脉冲[14]，ANTONELLI G A 提出了基于透射衍射光栅的空间分布调制技术[15]，裴翠祥发展了基于同一激光源的光纤束阵列传输时空调制方法[16]并研究了结构的超声响应规律。

本文基于双光束干涉形成的栅形空间调制，从数值分析及实验研究两方面研究了激光瞬态光栅作用于

基金项目：国家自然科学基金（No.62005311）
第一作者：姚东（1982—），男，副研究员，硕士，主要研究方向为结构健康监检测技术与超快诊断应用技术。Email：yaodong@opt.ac.cn
通讯作者：高贵龙（1985—），男，副研究员，博士，主要研究方向为超快诊断技术与全光固体光学技术。Email：gaoguilong@opt.ac.cn
收稿日期：2022-03-15；**录用日期**：2022-06-02

铝合金平板的结构响应特性,分析了相比于点源、线源等激发模式的优势。

1 激光瞬态光栅激励铝板的数值分析

1.1 热弹效应及其控制方程

对于金属等不透光材料,激光照射时存在反射及吸收等现象。激光瞬态光栅激励下,结构产生超声的热弹机制描述为:脉冲激光辐照材料表面后,激光一部分能量被材料表面反射、其余能量被表面吸收,使表面温度快速上升形成大的温度梯度产生热膨胀现象。

据热弹耦合理论,激光瞬态光栅的时域热弹波动方程表示为[17]

$$k\left(\frac{\partial^2 T}{\partial^2 x}+\frac{\partial^2 T}{\partial^2 y}\right)-\rho c\frac{\partial T}{\partial t}=Q \tag{1}$$

式中,k为热传导率,c为比热容,$T(x,y,t)$为温度,$Q(x,y,t)$为脉冲热源。脉冲激光热源可以表示为

$$Q=I_0 f(t)g(x)h(y) \tag{2}$$

式中,$f(t)$、$g(x)$、$h(y)$分别表示脉冲激光时间分布函数和脉冲激光空间分布函数,I_0是入射到材料表面的激光功率密度。I_0表示为

$$I_0=\frac{E}{\pi a_0^2 t_0} \tag{3}$$

式中,E是泵浦光束的激光入射能量。

脉冲激光激励的超声包含纵波、横波及表面波,其传播速度和材料的密度和弹性常数有关。根据固体力学理论,可知

$$C_{\mathrm{L}}=\sqrt{\frac{E}{\rho}}\sqrt{\frac{1-\mu}{(1+\mu)(1-2\mu)}} \tag{4}$$

$$C_{\mathrm{S}}=\sqrt{\frac{E}{\rho}}\sqrt{\frac{1}{2(1+\mu)}} \tag{5}$$

$$C_{\mathrm{R}}=\frac{0.87+1.13\mu}{1+\mu}C_{\mathrm{S}} \tag{6}$$

式中,C_{L}为纵波波速,C_{S}为横波波速,C_{R}为表面波波速,E为弹性模量,μ为泊松比,ρ为材料的密度。

1.2 仿真模型及参数

结构尺寸为50 mm×50 mm×5 mm,网格离散情况见图1,网格数量为189 062个,计算节点32 028个;在铝板上表面中心位置附近进行网格加密,并按一定范围进行过渡处理,以满足加载区域收敛及整体计算规模可控的综合要求。

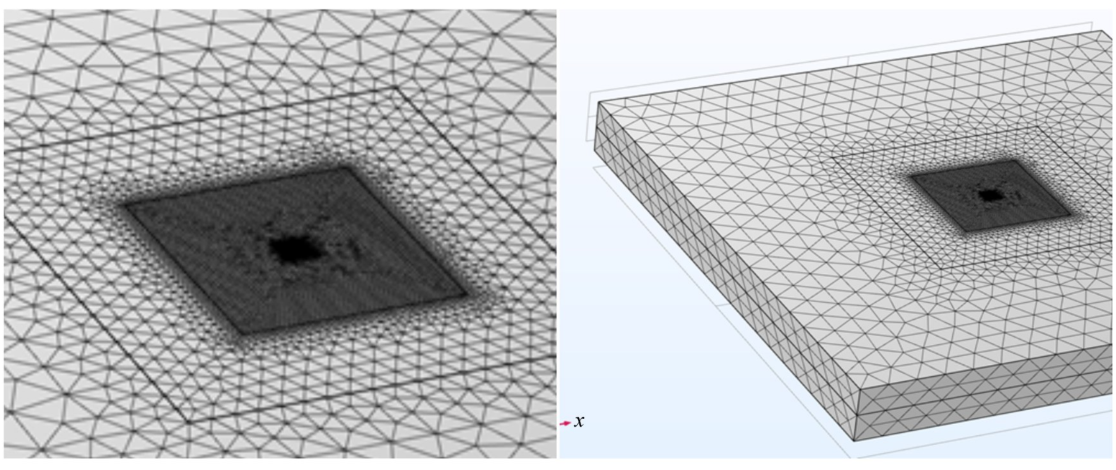

图1 网格离散情况

Fig. 1 Grid discrete case

参数取值见表1。

表1　参数取值

Table 1　Parameter value

Parameter	Specific heat capacity/ (J·kg^{-1}·K^{-1})	Thermal conductivity/ (W·m^{-1}·K^{-1})	Thermal expansivity/K^{-1}	Density/(kg·m^{-3})	Modulus of elasticity/MPa	Poisson′s ratio
Value	905	240	2.36×10^{-5}	2 700	70×10^{9}	0.33

1.3　结构粗糙表面对激光吸收率的分析

在激光处理与激光加工领域，针对粗造表面对激光的吸收过程，发展了反射-吸收综合模型和集总测试法等测定激光吸收率的方法。

本文按反射-吸收综合模型处理。对于一定的表面形貌，对其做倒三角下折处理，如图2所示[18]。

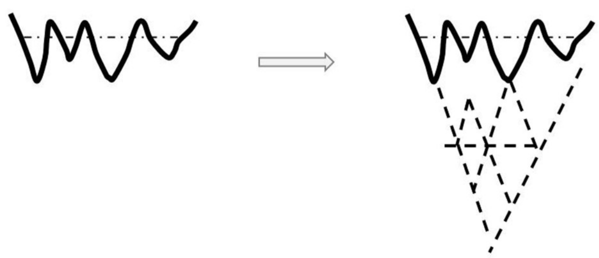

图2　粗糙表面的倒三角下折处理

Fig. 2　Treatment of rough surface with inverted triangle and downward folding

定义宏观尺度的取样长度L、轮廓算术平均偏差Ra(粗糙度)、波谷数N，则有等效粗糙度倾角θ满足

$$\tan\theta=(8\times \mathrm{Ra}\times N)/L \tag{7}$$

求解θ后，根据其数值大小落到的范围，可判定激光全反射的次数及占比，进而按理论公式获得吸收率A。

1)若$0<\theta\leqslant(\pi/6)$，为1次反射，A同垂直理想表面的吸收率。

2)若$(\pi/6)<\theta\leqslant(\pi/4)$，为全部1次反射、部分2次发射，$A$与入射角、垂直理想表面吸收率等相关。

本文采用表面粗糙度仪对所用铝合金上表面靠近中间位置进行了测试，结果为：粗糙度Ra=0.584 μm、波谷数N=94、取样长度L=287.3 μm。

求得吸收率为A=11.29%。

1.4　仿真结果分析

以脉冲宽度1 ns、单脉冲6 mJ为输入激光束斑，对应的瞬态激光光栅的直径为1 mm、条纹数量为11。结果提取时，均按图3部署观察点；其中，X方向为垂直于瞬态光栅条纹方向、Y方向为沿瞬态光栅条纹方向。

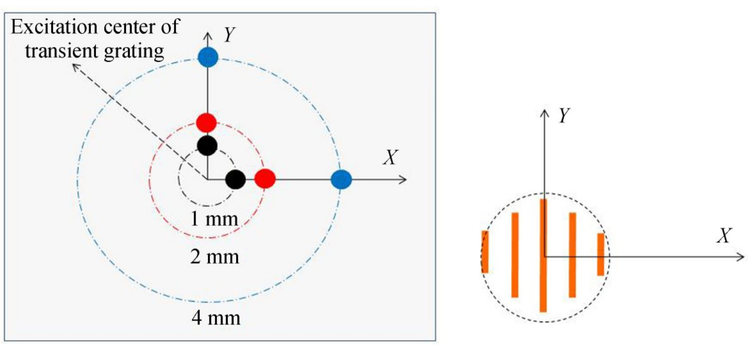

图3　观察点部署及参考系示意

Fig. 3　Observation point deployment and reference frame schematic

1)瞬态光栅激励的结果

图4为1 μs时刻的纵向位移云图,可以看出:a)以瞬态光栅作用区域为中心,其位移场呈现明显的“线阵列”特性,实现了传统点源激发、线源激发到本项目预期的线阵列激发;b)远场位移呈现环状分布,符合结构载荷的局部作用原理。

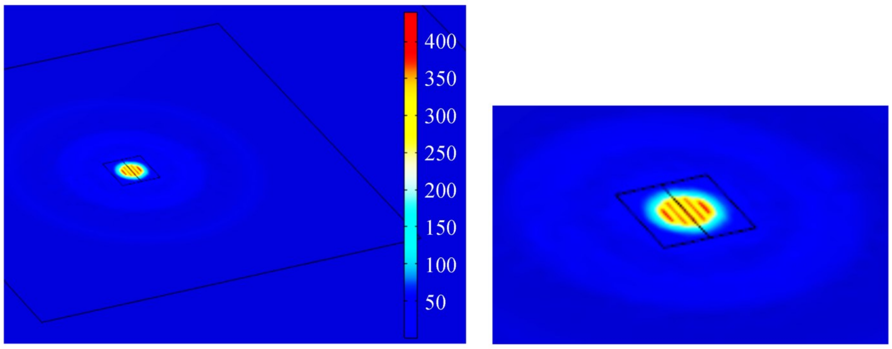

图4　1μs时刻的表面纵向位移云图

Fig. 4　Surface longitudinal displacement nephogram at time 1μs

图5为沿X轴、垂直于瞬态光栅方向,距离中心点1 mm、2 mm、4 mm、10 mm位置的纵向位移随时间的变化情况,比对表明:a)随着距离的增加,位移幅值降低、峰值时刻后延;b)各观测点的位移-时间响应规律均呈现先上升、后下降;图6为沿Y轴、垂直于瞬态光栅方向,距离中心点1 mm、2 mm、4 mm、10 mm位置纵向位移随时间的变化情况,其整体规律与沿X轴一致。

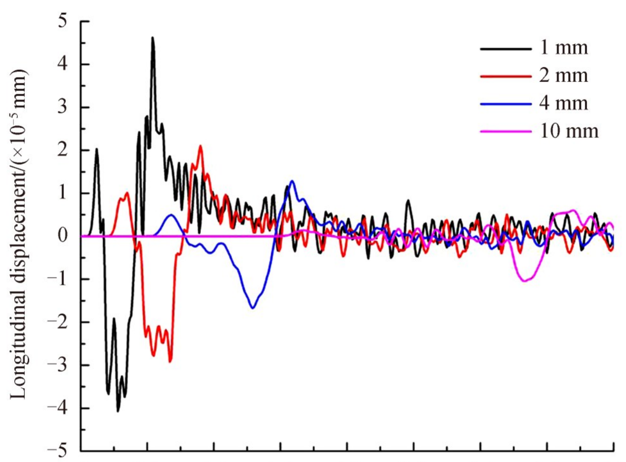

图5　沿X方向距离中心点不同距离处的纵向位移对比情况

Fig. 5　Comparison of longitudinal displacements at different distances from the center point along the X direction

为比对不同方向位移响应的特征,以图5所示沿X方向、图6所示沿Y方向数据为基础,取距离中心1 mm、2 mm、4 mm观测点,比对分析见图7:1)相同距离下,X方向与Y方向的响应规律,负向峰值略低;2)相同距离下,X方向峰值局部存在小幅震荡,Y方向的响应曲线更为光滑。

图7的分析表明,为避免局部震荡带来的检测难度,后续应观察位置沿Y方向部署。取图5以及图7中正向峰值、负向峰值及其时刻数据,见表2。

2)相同能量输入时传统点源/线源激发模式的结果

维持结构形式、材料性能以及激光脉宽不变,对点源、线源等传统激发模式进行仿真分析,并开展比对分析。其中:1)点源直径按0.1 mm,线源宽度按0.1 mm、长度按1 mm;2)点源、线源对应的功率,由线阵列6 mJ按面积均匀折算。

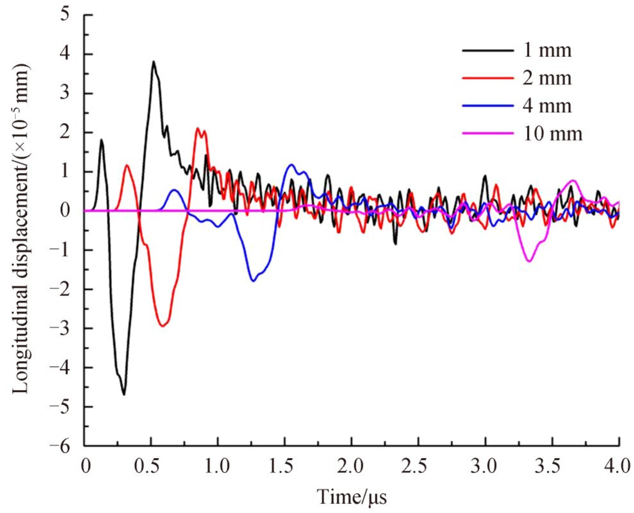

图6　沿 Y 方向距离中心点不同距离处的纵向位移对比情况

Fig. 6　Comparison of longitudinal displacements at different distances from the center point along the Y direction

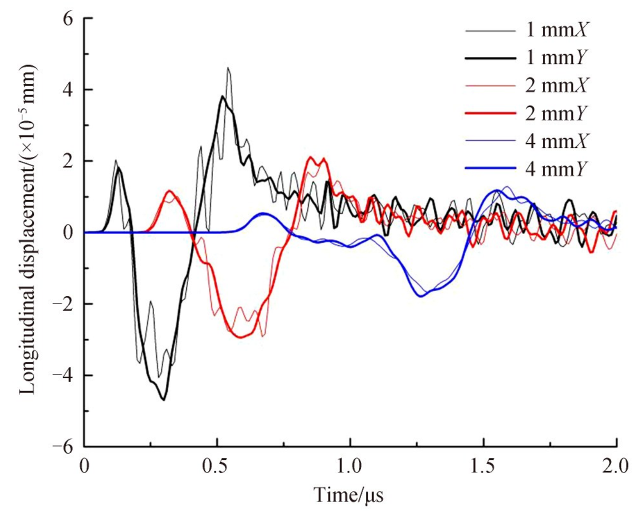

图7　不同方向位移响应的比对情况

Fig. 7　Comparison of displacement responses in different directions

表2　沿 X 轴、Y 轴不同距离处峰值位移数据

Table 2　Peak displacement data at different distances along X axis and Y axis

Distance along the X, Y axis/mm	1	2	4	10
Positive X displacement/mm	2.0527×10^{-5}	1.0331×10^{-5}	4.3491×10^{-6}	1.5711×10^{-6}
Moment/μs	0.12	0.35	0.76	1.70
Negative X displacement	4.0811×10^{-5}	2.4665×10^{-5}	1.6921×10^{-5}	1.1061×10^{-5}
Moment/μs	0.28	0.62	1.29	3.35
Positive Y displacement/mm	1.6937×10^{-5}	1.19109×10^{-5}	5.3182×10^{-6}	1.5077×10^{-6}
Moment/μs	0.13	0.32	0.68	1.69
Negative Y displacement	4.7071×10^{-5}	3.0451×10^{-5}	1.8527×10^{-5}	1.3078×10^{-5}
Moment/μs	0.30	0.59	1.26	3.33

考虑脉冲光栅特性对响应模式的影响,结合图7的分析结论,3类激发模式下均对沿 Y 方向设置且距离中心1 mm、2 mm、4 mm的观测点进行分析,见图8至图10。比对表明:1)初始时间段内的响应均呈现"正峰值-负峰值-正峰值"的规律;2)观测距离小于等于4 mm的范围内,位移响应的峰值大小依次为瞬态光栅激发、点源激发和线源激发,瞬态光栅激发下峰值为点源激发的2~5倍。

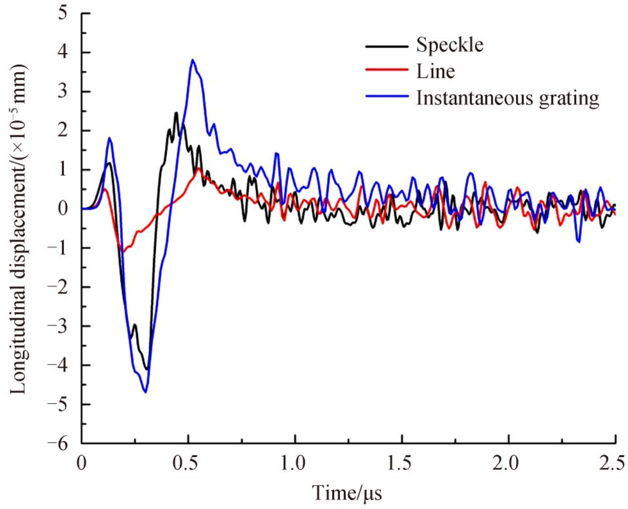

图8 3类激发模式下距离中心1 mm处的纵向位移对比

Fig. 8 Comparison of longitudinal displacements at 1 mm from the center under three excitation modes

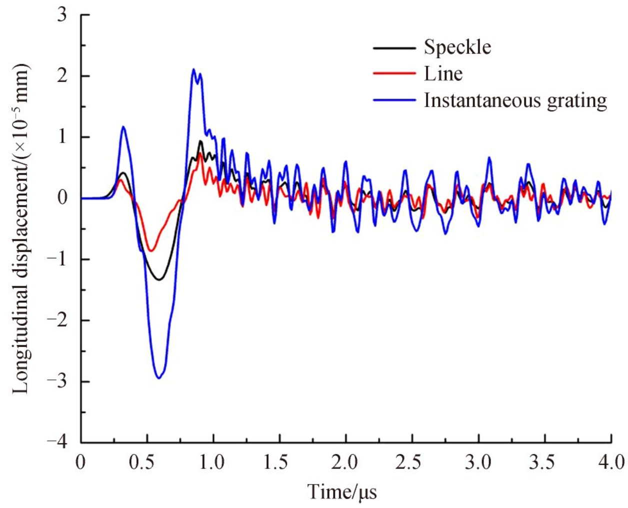

图9 3类激发模式下距离中心2 mm处的纵向位移对比

Fig. 9 Comparison of longitudinal displacements at 2 mm from the center under three excitation modes

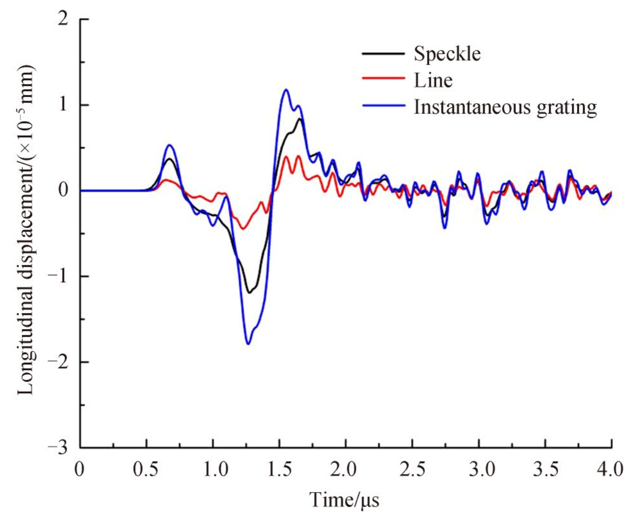

图10 3类激发模式下距离中心4 mm处的纵向位移对比

Fig. 10 Comparison of longitudinal displacements at 4 mm from the center under three excitation modes

表3列出了不同激发模式下，初始阶段“正峰值-负峰值-正峰值”的数值-时间数据，以及结构表面单位面积的能量。表3的数据表明：1）瞬态光栅激发模式下，靠近中心区域附近的响应程度显著优于传统的点源、线源激发模式，为提升信噪比奠定了良好基础；2）鉴于3类激发模式下总的输入能量一致，具备更大作用面积的瞬态光栅激发模式，大幅降低了结构表面单位面积的能量，从而远离激光热烧蚀阈值、具有更好的结构安全性。

表3　不同激发模式下特征数据比对

Table 3　Comparison of feature data in different excitation modes

Excitation mode	Energy density/ (mJ•mm^{-2})	Peak displacement			
		Observation point position/mm	Positive peak value 1	Negative peak value	Positive peak value 2
Point source	763.36	1	10.936	40.326	24.538
		2	4.113	13.278	9.195
		4	3.706	11.890	8.372
Linear source	60.00	1	4.122	1.116	10.098
		2	3.149	8.629	6.988
		4	1.218	4.442	3.983
Transient grating	7.64	1	16.937	47.071	38.143
		2	11.911	30.451	21.110
		4	5.318	18.527	11.616

2　激光瞬态光栅激励铝板的实验研究

2.1　实验原理及实验装置

图11为实验原理，脉冲激光器产生的激光束斑经瞬态光栅模块的分束、干涉，形成“亮暗”相间的激光瞬态光栅；激光瞬态光栅作用到铝板表面，经热弹效应在铝板内部激发超声波，超声波引起结构表面的纵向位移；采用激光干涉仪对距离光栅作用中心2 mm、10 mm的结构表面位移进行采集，采集信号由示波器展示。

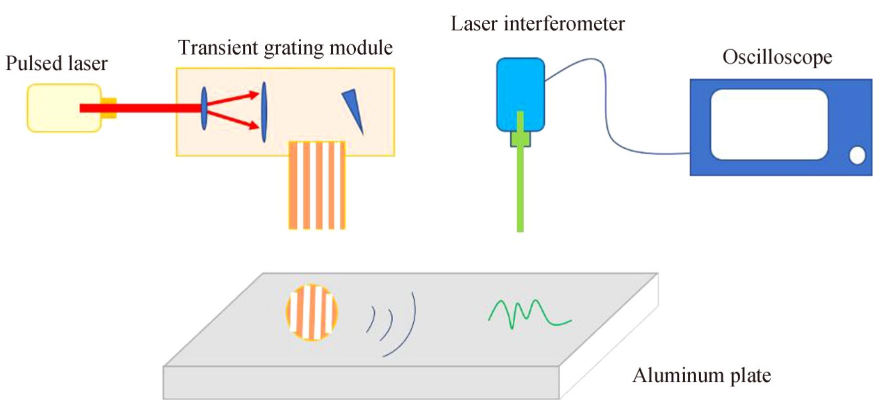

图11　激光瞬态光栅激励铝板的实验原理

Fig. 11　Experimental principle of laser transient grating excitation aluminum plate

实验装置含脉冲激光器、瞬态光栅模块、激光干涉仪、示波器及铝合金板。图12为布局情况以及光路示意。激光器用于产生脉冲激光。选用北京卓镭TINY-100L型，激光波长532 nm，重复频率10 Hz，单脉冲能量6 mJ，与仿真分析的参数选取一致。瞬态光栅模块对脉冲激光器产生的束斑进行展开，产生阵列化空间分布的瞬态光栅。该模块主要包括分束镜、光学延迟线、水平方向可调反射镜、光衰减器和合束镜等，输出光斑尺寸为直径1 mm、条纹数11，与仿真分析的参数选取一致。激光干涉仪用于检测结构表面的位移信号，选用Polytec.Inc公司VibroFlex Neo型。示波器选用Tektronic MDO3052型，采样率为500 MHz。铝合

金板吸收瞬态光栅能量后，经热弹效应产生超声波并在表面产生位移。实验选用市售ZL101，规格为49.36 mm×49.80 mm×4.97 mm。

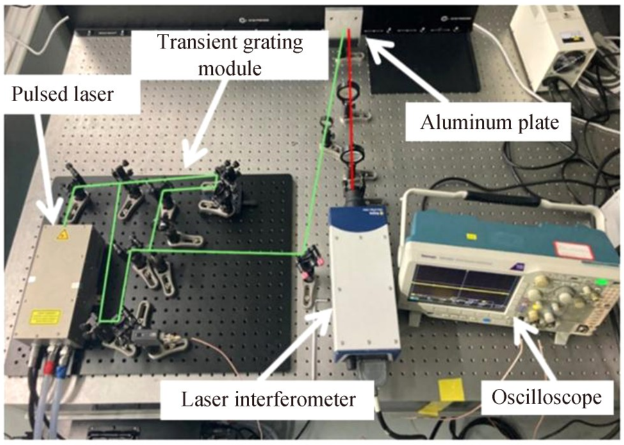

图12　实验装置布局情况以及激发-检测光路示意

Fig. 12　Experimental device layout and excitation - detection light circuit diagram

2.2　实验结果

提取示波器信号、将信号电压值转化为位移值后，经标定相对时延，得到位移数据见图13，噪声幅值约为1 nm。与仿真数据比对如图14所示，整体规律一致，峰值点数据的相对偏差最大值位于负向，约为8.81%。

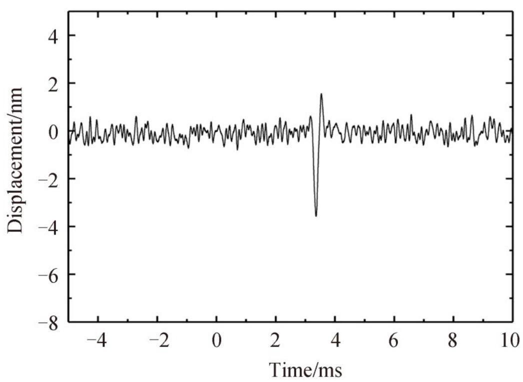

图13　瞬态光栅激发的位移数据原始值

Fig. 13　The original displacement data of transient grating excitation

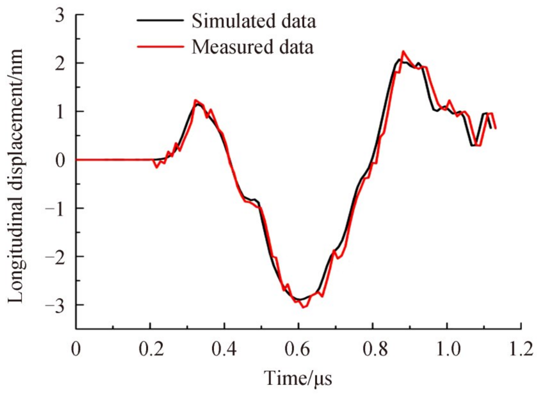

图14　观测点位移的实测与仿真数据比对情况

Fig. 14　Comparison between measured and simulated data of observation point displacement

同时，提取了距离光栅中心位置10 mm处的响应。其峰值的信号时延为3.35 μs；按10 mm布设距离，3.35 μs的峰值信号时延对应的声表面波速度2 974.3 m/s。由弹性波理论求得的速度为2 789.5 m/s，两者偏差为6.62%。

3　结论

仿真分析及实验验证表明，栅形激发技术通过分散降低单位面积的能级，并沿栅形方向形成了超声增强。对于距离中心相同距离的观测点，垂直于瞬态光栅方向与沿瞬态光栅方向的响应规律、峰值大小一致；相同距离下，垂直于瞬态光栅方向的响应存在峰值附近的小幅震荡，沿瞬态光栅方向的位移曲线更为光滑。为避免近场检测时因局部震荡的干扰，应将观察采样位置沿瞬态光栅方向部署。点源激发、线源激发以及瞬态光栅激发的位移响应均呈现"正峰值-负峰值-正峰值"的规律；小于等于4 mm的观测距离范围内，位移响应的峰值大小依次为瞬态光栅激发、点源激发和线源激发，瞬态光栅激发下峰值为点源激发的2～5倍，为

提升信噪比、减小近场盲区奠定了良好基础。鉴于3类激发模式下总的输入能量一致,瞬态光栅激发对应的结构表面能量密度约为点源模式的1%、线源模式的12.7%,可降低激光热烧蚀风险、具有更好的结构安全性。

参考文献

[1] GUO Hongtao, CAO Fuqi. Ultrasonic testing of the interface bonding quality of solid rocket motor charge[J]. Aero Weaponry,2006,(6):49-52.
郭洪涛,曹付齐.固体火箭发动机装药界面胶接质量超声波检测[J].航空兵器,2006,(6):49-52.

[2] SIMONETTI F. Localization of pointlike scatterers in solids with subwavelength resolution[J]. Applied Physics Letters, 2006, 89(9): 513-36619.

[3] LIU Jizhong, ZHOU Xiaojun, JIANG Zhifeng. Porosity test in carbon composites based on a new ultrasonic attenuation method[J]. Materials Science & Technology, 2007, (2): 260-263.
刘继忠,周晓军,蒋志峰.碳纤维复合材料孔隙率超声衰减测试研究[J].材料科学与工艺,2007,(2):260-263.

[4] LIU Songping, LIU Feifei, SHI Junwei, et al. High-resolution ultrasonic imaging evaluation and behavior analysis of impact damages in composites[J]. Journal of Mechanical Engineering, 2013, 49(22): 16-23.
刘松平,刘菲菲,史俊伟,等.复合材料冲击损伤高分辨率超声成像检测与损伤行为分析[J].机械工程学报,2013,49(22):16-23.

[5] MA Baoquan, ZHOU Zhenggan. Progress and development trends of composite structure evaluation using noncontact nondestructive testing techniques in aviation and aerospace industries[J]. Aero Weaponry, 2014, 35(7): 1787-1803.
马保全,周正干.航空航天复合材料结构非接触无损检测技术的进展及发展趋势[J].航空学报,2014,35(7):1787-1803.

[6] ZHOU Rui, LI Fengping, HONG Minghui. Laser interaction with materials and its applications in precision engineering[J]. Scientia Sinica: Physica, Mechanica & Astronomica, 2017, 47(2): 25-34.
周锐,李峰平,洪明辉.激光与物质相互作用及其精密工程应用[J].中国科学:物理学、力学、天文学,2017,47(2):25-34.

[7] WANG Yingze, ZAN Chen. Asymptotic analysis of heat transfer behavior of metal sheet irradiated by ultra-short pulse laser based on DPL model[J]. Journal of Jiangsu University(Natural Science Edition), 2020, 41(2): 243-248.
王颖泽,昝晨.基于DPL模型对超短脉冲激光辐照金属薄板传热行为的渐进分析[J].江苏大学学报(自然科学版),2020,41(2):243-248.

[8] LI Yibo, HAN Yi, YANG Guang, et al. Weak defect enhancement in ultrasonic testing of laser deposition manufactured TA15 alloys[J]. Chinese Journal of Lasers, 2018, 45(11): 69-76.
李一波,韩毅,杨光,等.激光超声检测激光沉积制造TA15合金弱小缺陷的增强[J].中国激光,2018,45(11):69-76.

[9] DENNETT C A, BULLER D L, HATTAR K, et al. Real-time thermomechanical property monitoring during ion beam irradiation using in situ transient grating spectroscopy[J]. Nuclear Instruments and Methods in Physics Research Section B: Beam Interactions with Materials & Atoms, 2019, 440: 126-138.

[10] YUAN Jiuxin, QIN Xunpeng, ZHANG Jinpeng, et al. Depth detection of internal defects for arc additive products based on laser ultrasound[J]. China Mechanical Engineering, 2021, 32(1): 65-73.
袁久鑫,秦训鹏,张进朋,等.基于激光超声的电弧增材制件内部缺陷深度检测[J].中国机械工程,2021,32(1):65-73.

[11] LU Minghui, DING Lei, YAN Xuejun, et al. Application and prospect of laser ultrasonic nondestructive testing technology in advanced manufacturing[J]. Journal of Vibration, Measurement & Diagnosis, 2021, 41(4): 631-643.
卢明辉,丁雷,颜学俊,等.激光超声技术在工业检测中的应用与展望[J].振动、测试与诊断,2021,41(4):631-643.

[12] SU Kun, REN Dahai, LI Jian, et al. Study on laser generating ultrasonic waves[J]. Opto-Electronic Engineering, 2002, 29(5): 68-72.
苏琨,任大海,李建,等.激光制声技术的研究[J].光电工程,2002,29(5):68-72.

[13] SONG Chao, ZHEN Bin, GUO Hualing, et al. Analysis of influence of light source on laser ultrasonic signal[J]. Journal of Applied Optics, 2017, 38(3): 494-498.
宋潮,郑宾,郭华玲,等.光源对激光超声信号特性的影响分析[J].应用光学,2017,38(3):494-498.

[14] NISHINO H, TSUKAHARA Y, NAGATA Y, et al. Optical probe detection of high-frequency SAWS generated by phase velocity scanning of laser interference fringes[J]. Japanese Journal of Applied Physics, 1994, 33: 3260-3264.

[15] ANTONELLI G A, ZANNITTO P, MARIS H J, et al. New method for the generation of surface acoustic waves of high frequency[J]. Physica B Physics of Condensed Matter, 2002, 2(2): 377-379.

[16] FEI Cuixiang, YI Dongchi, LIU Tianhao, et al. Enhanced laser ultrasonic detection method based on space time modulation[C]. Harbin: 2018 National Conference on Solid Mechanics, 2018.
裴翠祥,弋东驰,刘天浩,等.基于时空调制的增强型激光超声检测方法[C].哈尔滨:2018年全国固体力学学术会议,

2018.

[17] HUANG Qiaojian, LIU Xiaojun, ZHANG Shuyi. Influence of temperature on thermal diffusivity of double perovskite Sr_2FeMoO_6 studied by laser-induced transient thermal grating[J]. Acta Acustica, 2011, 36(2): 134-138.
黄巧建，刘晓峻，张淑仪. 利用瞬态热栅技术研究Sr_2FeMoO_6的热扩散系数及其温度效应[J]. 声学学报，2011，36(2)：134-138.

[18] CHEN Jun, ZHANG Qunli, YAO Jianhua, et al. Influence of surface roughness on laser absorptivity [J]. Laser Technology, 2008, 32(6): 624-627.
陈君，张群莉，姚建华，等. 材料表面粗糙度对激光吸收率影响的研究[J]. 激光技术，2008，32(6)：624-627.

Research on Ultrasonic Response Characteristics of Structures Excited by Laser Transient Grating

YAO Dong[1,4], GAO Bo[2], SONG Yingzheng[3], LI Qun[3], GAO Guilong[4]
(1 *Rocket Force University of Engineering*, *Xi'an* 710025, *China*)
(2 *Shanghai Academy of Spaceflight Technology*, *Shanghai* 200233, *China*)
(3 *Xi'an Jiaotong University*, *Xi'an* 710049, *China*)
(4 *Xi'an Institute of Optics and Precision Mechanics*, *Chinese Academy of Sciences*, *Xi'an* 710119, *China*)

Abstract: Ultrasonic Nondestructive Testing (NDT) supports field use and has a strong resolution, which is a key developing method in the field of structural health supervision and testing. In recent years, contact-type technical paths such as patch detection, medium coupling detection, and air coupling detection based on piezoelectric sensors have been formed, which are widely applied to many industries. With the integration of high-quality pulsed laser technology and the research on the mechanism of laser-matter interaction, the detection technology of pulsed laser-excited ultrasound has gradually developed. This technology is expected to solve the problems of surface pollution and fixed detection area caused by traditional piezoelectric-excited adhesive sensors and coating coupling agents. The ultrasonic wave excited by pulsed laser includes longitudinal wave, transverse wave and surface wave, and its propagation velocity is related to the density and elastic constant of the material. In the past, the spot source mode and line source mode of a pulsed laser beam, as well as the line source array mode modulated by lens array and fiber bundle with fixed physical structure, limited the flexibility of spatial expansion of pulsed laser, and also restricted the development of structural response characteristics and signal-structure correlation analysis under the new excitation mode. The disadvantages of pulsed laser excitation are: the monochromatic coherence of laser restricts the modulation ability of beam spot, which leads to the limitation of ultrasonic time-frequency mode, meanwhile, the structural damage threshold limits the energy of pulsed laser, which leads to the shortage of ultrasonic signal intensity. In this paper, the spatial expansion of pulsed laser is combined with laser ultrasonic nondestructive testing technology. Then, the structural response of laser transient grating acting on aluminum alloy plate is studied from two aspects: numerical analysis and experimental research by adopting the idea of numerical analysis to reveal the law and experimental research to verify the method. By deploying observation points at different distances and directions from the center of the grid excitation, the peak gain and the decrease of energy density of the grid excitation signal are obtained for the first time, and the direction angle of near-field enhancement is revealed. The structure size of the simulation model is 50 mm×50 mm×5 mm, the number of grids is 189 062, and the number of computing nodes is 32 028. Mesh encryption is carried out near the center of the upper surface of the aluminum plate, and transition treatment is carried out in a certain range to meet the comprehensive requirements of convergence of the loading area and controllable overall calculation scale. In the field of laser processing and laser processing, aiming at the laser absorption process of rough surface, the reflection-absorption comprehensive model and lumped test method are developed to measure the laser absorption rate. In terms of numerical analysis, the influence of surface roughness on absorptivity under the framework of reflection and absorption model was studied. The excitation process of laser transient grating with a 1mm diameter, 1ns pulse width and 6 mJ single pulse input was simulated, and the comparative analysis of point laser source and line laser source with the same energy was carried out. The numerical results show that the peak value of ultrasonic signal under transient grating excitation was 2～5 times that of point source excitation when the observation distance less than or equal to 4 mm, and the surface energy density of the structure was about 1% of that excited by point source and 12.7% of that excited by line source. The principle of the experiment is that the laser beam spot generated by the pulse laser is split and interfered with by the transient grating module, then, a "bright and dark" laser transient grating is formed. The transient laser grating acts on the surface of the aluminum plate, and the ultrasonic wave is excited in the aluminum plate by thermoelastic effect, which causes the longitudinal displacement of the structural surface. The laser interferometer is used to collect the displacement of the structure surface which is 2 mm and 10 mm away from the center of grating action, and the collected signal is displayed by oscilloscope. The device includes pulse laser, transient grating module, laser interferometer, oscilloscope and aluminum alloy plate. In terms of experimental research, the transient grating module was developed, and the laser transient grating ultrasonic experiments were performed on aluminum plate. The experimental results show that the amplitude of ultrasonic was about 1 nm under 60 kHz high pass filtering, the maximum relative deviation of the surface displacement peak was 8.91%, and the deviation of surface acoustic wave velocity was 6.62%, corresponding to the signal delay at 10 mm from the center of the grating. Synthesize the above analysis, the dispersion of laser beam spot excited by laser transient grating reduces the energy density per unit area of the structure surface, and forms ultrasonic enhancement along the grating direction, which lays a good foundation for improving the signal-to-noise ratio and ensuring the safety of the structure.

Key words: Ultrasonic nondestructive testing; Laser excitation; Grating spatial modulation; Energy density; Signal intensity

OCIS Codes: 140.3460; 050.2770; 120.4290; 070.7345

Foundation item: National Natural Science Foundation of China (No. 62005311)